Available online at www.sciencedirect.com
SCIENCE DIRECT
Polymer 47 (2006) 4925–4935
polymer
www.elsevier.com/locate/polymer

Synthesis and characterization of novel monomers and polymers containing chiral (−)-menthyl groups

Jui-Hsiang Liu *, Po-Chih Yang

Department of Chemical Engineering, National Cheng Kung University, No. 1, University Road, Tainan 70101, Taiwan, ROC

Received 3 April 2006; received in revised form 12 May 2006; accepted 15 May 2006
Available online 6 June 2006

Abstract

To investigate the steric effects of chiral menthyl groups on the induction of cholesteric liquid crystals and the sensitivity of the photoisomerizable azobenzene derivatives, a series of chiral monomers and a photoisomerizable chiral azobenzene derivative with various spacers end-capped with (−)-menthyl group were synthesized. The structures of the novel chiral compounds synthesized in this investigation were identified using ^{13}C NMR, FTIR, and elemental analysis. The phase transition temperatures of the chiral compounds were investigated using X-ray diffraction, differential scanning calorimetry, and polarizing optical microscopy. The thermogravimetric characteristics, the glass-transition temperatures (T_g) and the weight–average molecular weights (M_w) of the homopolymers were also evaluated. Polymers containing chiral menthyl groups with a biphenyl segment were found to reveal high thermal resistance. However, the existence of the steric hindered menthyl group disturbed the arrangement of chiral monomers leading to the disappearance of liquid crystal phases. The specific optical rotation of the synthesized monomers and polymers were also evaluated. The effect of the synthesized chiral compounds, monomers and photoisomerizable azobenzene derivative on the induction of the cholesteric liquid crystal films was investigated. The morphological network structure of the polymer matrix inside a liquid crystal cell was studied using a scanning electron microscope (SEM). The phototuning ability of the AzoM on the cholesteric liquid crystals was also established.

Keywords: Chiral polymers; Cholesteric; Liquid crystal

1. Introduction

Systematic investigations of the synthesis, characterization and applications of side chain liquid crystalline polymers began only after Ringsdorf [1] and others proposed that a flexible spacer should be inserted between the polymeric main chain and the mesogenic side groups to decouple the motions of the main chain and side groups in the liquid crystalline state. Since, Ringsdorf et al. developed the first side chain liquid crystal polymers in 1978; research in polymer liquid crystalline science and its technological applications has dramatically increased [2–7]. Recently, a new approach for the development of chiral nematic (or cholesteric) low molar mass [8–11] and polymeric materials showing light-induced and controllable changes in the helical pitch lengths has been reported [12–14]. This approach is based on the introduction of chiral photosensitive fragments into the nematic matrix. These fragments undergo light-induced E–Z photoisomerization. As a result of this process, Z-isomerization of the chiral photochromic groups takes place. This isomerization is accompanied by a decrease in the anisometry of the photochromic groups and, as a consequence, results in a decrease in their helical twisting power (HTP). Therefore, upon light irradiation, the macroscopic chirality of the system is reduced and, in the case of systems containing a single chiral component, the helical pitch length increases. Such systems appear to be quite attractive from the viewpoint of their practical application potential, because, upon light irradiation and the concurrent untwisting of the cholesteric helix, the selective light reflection maximum is shifted to the longer wavelength region of the spectrum. Hence, the optical properties of films based on such systems may be easily controlled by light irradiation via local variations in the selective light reflection wavelength.

In recent years, there have been many publications devoted to the study of the preparation and the applications of photosensitive liquid crystal polymer composed of chiral terminal moiety [15,16]. Photocontrollable cholesteric polymers introduce photosensitive or photoisomerized mesogenic

* Corresponding author. Tel.: +886 6 2757575; fax: +886 6 2384590.
E-mail address: jhliu@mail.ncku.edu.tw (J.-H. Liu).

0032-3861/$ - see front matter © 2006 Elsevier Ltd. All rights reserved.
doi:10.1016/j.polymer.2006.05.043

fragments such as azobenzene and stilbene, which could reverse their configuration when irradiated with different light wavelengths. When the configuration of the polymer changes, the twisting power or optical characteristics also changes at the same time. Composite films are photoirradiated at different wavelengths to bring about the photoisomerization of the guest azobenzene. Azobenzene is an attractive photosensitive material because of its simple photochemistry and ease of chemical modification. Azobenzene dissolved in a chiral nematic (cholesteric) liquid crystal provides photocontrollability of the helical pitches as a result of E–Z photoisomerization, as demonstrated by Sackmann [17]. On the other hand, a chiral azobenzene derivative dissolved in a nematic liquid crystal can act as a chiral dopant to induce a chiral nematic phase and a phototrigger to control the generated helical pitch [18].

The synthesis of a series of chiral dopants and chiral polymers were investigated in our previous papers [19–22]. Their optical properties and applications on the liquid crystal cells and recording films were also studied. In this paper, a series of chiral monomers and an azobenzene derivative containing chiral (−)-menthyl moiety were synthesized. The thermal properties and specific rotation of chiral monomers, azobenzene derivative, and chiral polymers were evaluated. Liquid crystal phases were studied through polarized optical microscopy (POM) and were conformed by using X-ray diffraction method. To investigate the chiral effect of the menthol moieties on the liquid crystals, menthyl 4-hydroxybenzoate was used to induce the cholesteric liquid crystal phase. Morphology of the polymer matrix inside the liquid crystal cells was studied. Photochemical tuning capability of the cholesteric liquid crystal cell with an azobenzene derivative was also evaluated.

2. Experimental

2.1. Measurements

FTIR spectra were recorded on a Jasco VALOR III (Tokyo, Japan) FTIR spectrophotometer. Nuclear magnetic resonance (NMR) spectra were obtained using a Bruker AMX-400 (Darmstadt, Germany) high-resolution NMR spectrometer. The optical rotation of chiral compounds was measured with a Jasco DIP-370 polarimeter using the D-line of sodium (λ = 589 nm). Measurements were performed using 1% solutions of substances in $CHCl_3$ (chloroform). Elemental analyses were conducted with a Heraeus CHN-O (Darmstadt, Germany) rapid elemental analyzer. Gel permeation chromatography (GPC) measurements were carried out at 40 °C on a Hitachi L-4200 (Osaka, Japan) instrument equipped with TSK gel GMH and G2000H columns using $CHCl_3$ as an eluent and the rate of the elution was 1.0 ml min^{-1}; the instrument was calibrated with a poly-styrene standard. Differential scanning calorimeter (DSC) was conducted with a Perkin–Elmer DSC 7 at a heating and cooling rate of 10 K min^{-1} in the nitrogen atmosphere. Thermal decomposition temperature data were recorded with a thermogravimetric analyzer (TGA) Perkin–Elmer TGA 7. The phase transitions were investigated by an Olympus BH-2 polarized light microscope (POM) equipped with Mettler hot stage FP-82 and the temperature scanning rate were determined at a rate of 5 K min^{-1}. The nanoparticle cluster distribution was estimated using a Jeol JSM-35 scanning electron microscope. UV spectroscopy measurements were carried out with a Jasco V-550 UV–vis spectrophotometer. The X-ray diffraction data was recorded on a Rigaku RINT 2500 series with Ni-filtered Cu Kα radiation. The sample in a quartz capillary was held in a temperature-controlled cell (Rigaku LC high-temperature controller).

2.2. Synthesis of monomers

Synthetic routes for the target monomers and chiral compounds are shown in Schemes 2 and 3. The following novel chiral monomers were synthesized according to the similar procedures described in the literature [23–26]. Compounds **1** and **2** were synthesized following the processes reported in the literature [26]. The obtained products were purified and then identified using FTIR and ^1H NMR.

2.2.1. 4-(6-Hydroxyhexyloxy) benzoic acid (*1*)

Yield: 19.1 g (67%), T_m = 139–140 °C. FTIR (cm^{-1}): 3249 (OH), 2932, 2856 (CH_2), 1685 (C=O in Ar-COO–), 1600, 1521 (C–C in Ar), 1287, 1251 (COC), 2681, 2561 (COOH). ^1H NMR (DMSO-d_6, δ in ppm): 1.28–1.74 (m, 8H, CH_2), 3.32 (m, 2H, OCH_2CH_2), 4.01 (m, 2H, CH_2OPh), 6.99–7.87 (m, 4H, aromatic), 12.6 (1H, –COOH).

2.2.2. 4-(6-Acryloyloxyhexyloxy) benzoic acid (*2*)

Yield: 6.3 g (69%), K 88 °C N 92 °C I. FTIR (cm^{-1}): 2933, 2854 (CH_2), 1733 (C=O in Ar-COO–), 1604, 1528 (C–C in Ar), 1291, 1246 (COC), 2672, 2566 (COOH), 1685 (C=C). ^1H NMR (DMSO-d_6, δ in ppm): 0.94–1.28 (m, 8H, CH_2), 4.05 (m, 2H, CH_2OPh), 4.12 (m, 2H, $COOCH_2$), 5.44 (dd, 1H, CH_2=CH), 5.68 (dd, 1H, CH), 5.86 (dd, 1H, CH_2=CH), 6.53–7.40 (m, 4H, aromatic), 12.5 (1H, –COOH).

2.2.3. 4-Menthyl 4-(6-acryloyloxyhexyloxy) benzoate (*3*)

Compound **2** (2.92 g, 10.0 mmol) and (L)-menthol (2.34 g, 15.0 mmol) was dissolved in CH_2Cl_2 (40 ml) at 30 °C. *N*,*N*′-Dicyclohexyl carbodiimide (DCC) (3.09 g, 15.0 mmol) and *N*,*N*′-dimethyl-aminopyridine (DMAP) (0.12 g, 1 mmol) were dissolved in CH_2Cl_2 (30 ml), and then added to the solution. The reaction mixture was stirred for 2 days at 30 °C. The resulting solution was filtered and washed with water, dried with anhydrous $MgSO_4$, and evaporated to dryness. The crude product was purified by column chromatography (silica gel, dichloromenthane, CH_2Cl_2). Yield: 2.45 g (57%). T_m = 10.4 °C. FTIR (cm^{-1}): 2930, 2869 (CH_2), 1732 (C=O in Ar-COO–), 1604, 1510 (C–C in Ar), 1257, 1198 (COC), 1638 (C=C). ^1H NMR ($CDCl_3$, δ in ppm): 0.86–0.96 (m, 9H, CH_3), 1.26–1.42 (m, 17H, CH_2), 4.0 (d, 2H, CH_2OPh), 4.17 (d, 2H, $COOCH_2$), 4.90 (m, 1H, $OCHCH_2$), 5.81 (dd, 1H, CH_2=CH), 6.12 (dd, 1H, CH_2=CH), 6.38 (dd, 1H, CH_2=CH), 6.90 (d, 2H, aromatic), 7.98 (d, 2H, aromatic).

*2.2.4. 4-(6-Hydroxyhexyloxy) biphenyl-4′-carboxylic acid (**4**)*

4-(4-Hydrophenyl) benzoic acid (15.0 g, 70.0 mmol) was dissolved in dimethylacetamide (DMAc, 50 ml). A solution of KOH (11.7 g, 210.0 mmol) and a catalytic amount of KI dissolved in DMAc (50 ml) and H_2O (8 ml) was added dropwise to the solution. 1-Chloro-hexanol (14.2 g, 105.0 mmol) was then added, and the solution was heated to 100 °C for 48 h. The resulting mixture was poured into water and extracted with ethyl ether. The water phase solution was acidified with HCl diluted with water until it was weakly acidic. The resulting precipitate was filtered off and washed several times with water. The crude product was recrystallized from EtOH/H_2O (4/1). Yield: 12.5 g (57%). T_m = 200–201 °C. FTIR (cm^{-1}): 3227 (OH), 2932, 2851 (CH_2), 1684 (C=O in Ar-COO–), 1600, 1506 (C–C in Ar), 1289, 1251 (COC), 2686, 2556 (COOH). ^{1}H NMR (*d*-acetone, δ in ppm): 1.42–1.84 (m, 8H, CH_2), 3.54 (m, 2H, OCH_2CH_2), 4.06 (m, 2H, CH_2OPh), 7.03 (d, 2H, aromatic), 7.58 (d, 2H, aromatic), 7.70 (d, 2H, aromatic), 8.06 (d, 2H, aromatic).

*2.2.5. 4-(Acryloyloxyhexyloxy) biphenyl-4′-carboxylic acid (**5**)*

Compound **4** (12.0 g, 38.2 mmol), *N*,*N*-dimethylaniline (5.0 g, 42.0 mmol), and a catalytic amount of 2,6-di-*tert*-butyl-4-methylphenol was dissolved in distilled 1,4-dioxane (70 ml). The solution was cooled with an ice/salt bath and then acryloyl chloride (10.3 g, 114.6 mmol) dissolved in distilled 1,4-dioxane (30 ml) was added dropwise under vigorous stirring. After the reaction mixture was stirred for 24 h at room temperature, the solution was poured into cold water and the precipitate was filtered. The crude product was washed several times with water and recrystallized twice from EtOH. Yield: 10.1 g (72%). T_m = 140–141 °C. FTIR (cm^{-1}): 2933, 2854 (CH_2), 1733 (CO in Ar-COO–), 1604, 1528 (C–C in Ar), 1291, 1246 (COC), 2672, 2566 (COOH), 1685 (C=C). ^{1}H NMR (DMSO, δ in ppm): 1.34–1.76 (m, 8H), 4.01 (m, 2H, CH_2OPh), 4.18 (m, 2H, $COOCH_2$), 5.90 (dd, 1H, CH_2=CH), 6.16 (dd, 1H, CH_2=CH), 6.32 (dd, 1H, CH_2=CH), 7.03 (d, 2H, aromatic), 7.65 (d, 2H, aromatic), 7.74 (d, 2H, aromatic), 7.97 (d, 2H, aromatic).

*2.2.6. Menthyl 4-(acryloyloxyhexyloxy) biphenyl -4′-carboxylate (**6**)*

Compound **5** (3.68 g, 10.0 mmol) and (L)-menthol (2.34 g, 15.0 mmol) was dissolved in CH_2Cl_2 (70 ml) at 30 °C. *N*,*N*′-Dicyclohexylcarbodiimide (DCC) (3.09 g, 15.0 mmol) and *N*,*N*′-dimethyl-aminopyridine (DMAP) (0.12 g, 1 mmol) were dissolved in CH_2Cl_2 (50 ml), and then added to the solution. The reaction mixture was stirred for 2 days at 30 °C. The resulting solution was filtered and washed with water, dried with anhydrous $MgSO_4$, and evaporated to dryness. The crude product was purified by column chromatography (silica gel, dichloromenthane, CH_2Cl_2) and recrystallized twice from EtOH. Yield: 2.38 g (47%). T_m = 60.5 °C. FTIR (cm^{-1}): 2931, 2856 (CH_2), 1730 (CO in Ar-COO–), 1608, 1524 (C–C in Ar), 1285, 1240 (COC), 1697 (C=C). ^{1}H NMR ($CDCl_3$, δ in ppm): 0.79–0.94 (m, 9H, CH_3), 0.92–2.16 (m, 17H), 4.01 (m, 2H, CH_2OPh), 4.18 (m, 2H, $COOCH_2$), 4.94 (m, 1H, $OCHCH_2$), 5.81 (dd, 1H, CH_2=CH), 6.12 (dd, 1H, CH_2=CH), 6.40 (dd, 1H, CH_2=CH), 6.97 (d, 2H, aromatic), 7.55 (d, 2H, aromatic), 7.61 (d, 2H, aromatic), 8.07 (d, 2H, aromatic).

*2.2.7. 4-(Methoxycarbonyloxy) benzoic acid [27] (**7**)*

4-Hydroxybenzoic acid (13.8 g, 0.1 mol) was added to a solution of 0.3 mol of sodium hydroxide in 0.5 l of water/ice mixture while stirring. Then methyl chloroformate (16.07 g, 0.17 mol) was slowly added to the resulting solution, which was maintained at 0 °C. The reaction mixture was stirred for a further 8 h and acidified to pH 4–5 by adding concentrated HCl. The precipitate was filtered off and recrystallized from ethanol. Yield: 16.1 g (82.1%). T_m = 175 °C. FTIR (cm^{-1}): 2961, 2895 (CH_2), 1693 (C=O in Ar-COO–), 1608, 1503 (C–C in Ar), 2680, 2555 (COOH). ^{1}H NMR (*d*-acetone, δ in ppm): 3.85 (m, 3H, CH_3O), 7.34 (d, 2H, aromatic), 8.12 (d, 2H, aromatic), 10.16 (COOH).

*2.2.8. Menthyl 4-(methoxycarbonyloxy) benzoate (**8**)*

Thionyl chloride (8 ml) was mixed with compound **7** (7.84 g, 40.0 mmol) and 1 ml of dimethylformamide in 30 ml dichloromethane and the solution was heated under reflux for 2 h. The excess of thionyl chloride was removed by evaporation. A solution of acid chloride (7.72 g, 36 mmol) in 30 ml of dichloromethane was slowly added to a solution of (L)-menthol (2.34 g, 15.0 mmol) in 30 ml of dichloromethane and 20 ml of pyridine. The reaction mixture was stirred for 1 day at room temperature. It was then washed with an aqueous solution of HCl (50 ml, 10%), and evaporated to dryness. Yield: 5.43 g (45.2%). FTIR (cm^{-1}): 2950, 2875 (CH_2), 1705 (C=O in Ar-COO–), 1608, 1503 (C–C in Ar). ^{1}H NMR ($CDCl_3$, δ in ppm): 0.84–0.96 (m, 9H, CH_3), 0.98–1.86 (m, 9H, CH_2), 3.79 (m, 3H, CH_3O), 4.94 (m, 1H, $OCHCH_2$), 7.24 (d, 2H, aromatic), 8.26 (d, 2H, aromatic).

*2.2.9. Menthyl 4-hydroxybenzoate (**9**)*

Compound **8** (5.01 g, 15 mmol) was stirred in a mixture of 30 ml ethanol and 30 ml aqueous ammonia (27%) at room temperature for 1 h, and then poured into water (50 ml), acidified with glacial acetic acid and shaken with diethyl ether. The organic layer was washed with water and dried over anhydrous $MgSO_4$. The ether was removed by evaporation and the product was purified by column chromatography (silica gel, ethyl acetate/hexane = 1/5) and recrystallized twice from EtOH. Yield: 2.64 g (67.2%), T_m = 92.5 °C. FTIR (cm^{-1}): 3347 (OH), 2947, 2872 (CH_2), 1686 (C=O in Ar-COO–), 1602, 1511 (C–C in Ar), 1220, 1281 (COC). ^{1}H NMR (*d*-acetone, in ppm): 0.78–0.90 (m, 9H, CH_3), 0.92–1.88 (m, 9H, CH_2) 4.82–4.90 (m, 1H, $OCHCH_2$), 6.88–6.91 (m, 2H, aromatic), 7.86–7.90 (m, 2H, aromatic).

*2.2.10. Menthyl 4-(6-acryloyloxyhexyloxy) phenyl -4′-benzoate (**10**)*

Compound **10** was synthesized following the method described in the literature [25]. To compare with other novel polymers containing pendant (−)-menthol group,

polymerization of the monomeric compound **10** and the physical properties of the obtained chiral polymer **P3** were all studied. Yield: 1.85 g (42.0%). T_m = 32.6 °C. FTIR (cm^{-1}): 2934, 2870 (CH_2), 1712 (C=O in Ar-COO–), 1610, 1505 (C–C in Ar), 1196, 1230 (COC), 1630 (C=C). ^1H NMR ($CDCl_3$, δ in ppm): 0.77–0.82 (m, 9H, CH_3), 0.89–1.91 (m, 17H, CH_2), 4.04 (d, 2H, CH_2OPh), 4.18 (d, 2H, $COOCH_2$), 4.90–4.97 (m, 1H, $OCHCH_2$), 6.96–6.99 (m, 2H, aromatic), 7.26–7.29 (m, 2H, aromatic), 8.01–8.16 (m, 4H, aromatic).

2.2.11. Menthyl [4-(6-acryloyloxyhexyloxy) biphenyl-4′ -carbonyloxy] benzoate (*11*)

Compound **5** (1.84 g, 5.0 mmol) and compound **9** (1.65 g, 6.0 mmol) were dissolved in CH_2Cl_2 (80 ml) at 30 °C. DCC (2.26 g, 7.5 mmol) and DMAP (0.06 g, 0.5 mmol) were dissolved in CH_2Cl_2 (40 ml) and then added to the former solution. The reaction mixture was stirred at 30 °C for 2.5 days. The resulting solution was filtered and washed with water, dried over anhydrous $MgSO_4$, and then evaporated. The crude product was purified by column chromatography (silica gel, dichloromenthane, CH_2Cl_2) and recrystallized twice from EtOH. Yield: 2.20 g (70.4%). T_m = 98.3 °C. FTIR (cm^{-1}): 2942, 2865 (CH_2) 1720 (C=O in Ar-COO–), 1615, 1508 (C–C in Ar), 1265, 1230 (COC), 1632 (C=C). ^1H NMR ($CDCl_3$, δ in ppm): 0.77–0.89 (m, 9H, CH_3), 0.92–2.06 (m, 17H, CH_2), 4.03 (d, 2H, CH_2OPh), 4.18 (d, 2H, $COOCH_2$), 4.90–4.99 (m, 1H, $OCHCH_2$), 6.99–7.02 (m, 2H, aromatic), 7.29–7.32 (m, 2H, aromatic), 7.58–7.71 (m, 4H, aromatic), 8.12–8.25 (m, 4H, aromatic).

2.2.12. 4-Hydroxy-4′-ethoxycarbonyl azobenzol (*12*)

Ethyl 4-aminobenzoate (10 g, 60.6 mmol) was dissolved in 1 M aqueous HCl (100 ml) kept in the ice bath at 0 °C. $NaNO_2$ (4.2 g, 60.8 mmol), dissolved in water (30 ml), was added dropwise to the solution and stirred for 30 min. Sodium hydroxide (7.2 g, 0.18 mol) and phenol (5.8 g, 61.7 mmol) were dissolved in water (80 ml) and then stirred for 30 mm at 0 °C; then, the former solution was added dropwise to the latter solution. The temperature was kept at 0 °C and stirred for 1 h. The resulting mixture was poured into water and the solution was neutralized with 5% aqueous HCl. The precipitated crude product was filtered and recrystallized twice from ethanol. Yield 11.8 g (72%). T_m = 153–154 °C. FTIR (cm^{-1}): 3399 (OH), 2973, 2927, 2906 (CH_2), 1693 (C=O in Ar-COO–), 1601, 1504 (C–C in Ar). ^1H NMR ($CDCl_3$, δ in ppm): 1.38 (t, 3H, OCH_2CH_3), 4.35 (d, 2H, OCH_2), 7.03–8.17 (m, 8H, aromatic).

2.2.13. Ethyl 4-(4-undecyloxyphenylazo) benzoate (*13*)

Compound **12** (8.1 g, 30 mmol) was dissolved in DMF (70 ml). Potassium hydroxide (2.52 g, 45 mmol), dissolved in DMF (50 ml), was added dropwise to the solution. Potassium iodide (0.83 g, 5 mmol) and 1-bromo-undecane (7.76 g, 33 mmol), dissolved in DMF (20 ml), was then added.

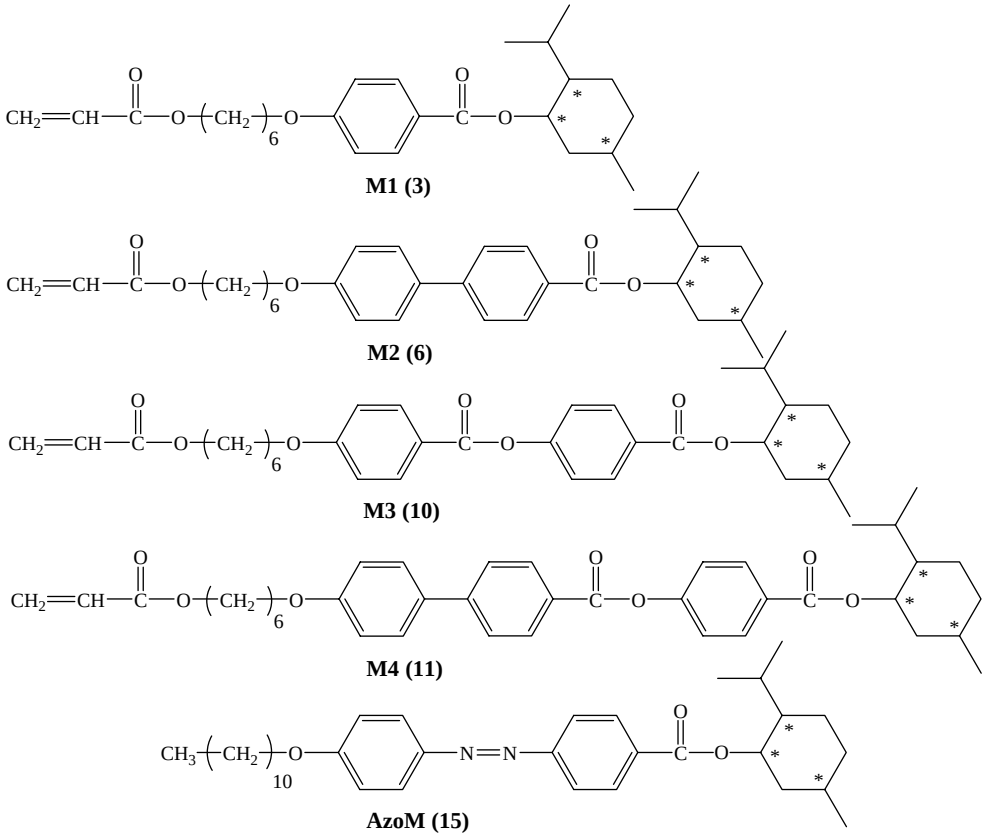

Scheme 1.

The solution was heated to 80 °C and kept at that temperature for 24 h with stirring. The resulting mixture was poured into water and extracted twice with $CHCl_3$. After evaporation, the crude product was recrystallized twice from ethanol. Yield: 9.42 g (74%). K 90.0 °C S_A 96.3 °C I (cooling). FTIR (cm^{-1}): 2950, 2855 (CH_2), 1690 (C=O in Ar-COO–). ^1H NMR (acetone-d_6, δ in ppm): 0.85–0.90 (m, 3H, CH_3), 1.08–1.24 (m, 18H, –CH_2), 1.37–1.40 (t, 3H, OCH_2CH_3), 4.02 (d, 2H, OCH_2Ph), 4.15 (d, 2H, OCH_2), 7.05–7.08 (d, 2H, aromatic), 7.78–7.92 (m, 4H, aromatic), 8.12–8.16 (d, 2H, aromatic).

2.2.14. 4-(4-Undecyloxyphenylazo) benzoic acid (**14**)

Compound **13** (10.6 g, 25.0 mmol) was dissolved in ethanol (60 ml). Potassium hydroxide (10 g, 178.5 mmol), dissolved in ethanol, was then added and the mixture was heated at reflux for 6 h. The resulting suspension was poured into water, and the solution was neutralized with dilute HCl. The solution was extracted twice with $CHCl_3$, washed with water, dried over magnesium sulfate, and evaporated. Yield: 8.03 g (81.0%). FTIR (cm^{-1}): 2945, 2852 (CH_2), 1689 (C=O in Ar-COO–). ^1H NMR (acetone-d_6, δ in ppm): 0.87–1.97 (m, 21H, –$C_{10}H_{21}$), 4.04 (d, 2H, OCH_2Ph), 7.10–7.12 (d, 2H, aromatic), 7.86–7.94 (m, 4H, aromatic), 8.12–8.14 (d, 2H, aromatic).

2.2.15. Menthyl 4-(4-undecyloxyphenylazo) benzoate (**15**)

Compound **14** (3.96 g, 10 mmol) and (L)-menthol (2.34 g, 15.0 mmol) were dissolved in CH_2Cl_2 (30 ml) at room temperature: DCC (3.09 g, 15.0 mmol) and DMAP (0.12 g, 1 mmol) were then added to the solution. The mixture was stirred for 24 h at 30 °C. The resulting mixture was then washed with water, dried over $MgSO_4$, and evaporated. The crude product was purified by column chromatography (silica gel, ethyl acetate/hexane = 1/5) and recrystallized from ethanol. Yield: 1.76 g (33.0%). T_m = 71.7 °C. FTIR (cm^{-1}): 2954, 2860 (CH_2), 1702 (C=O in Ar-COO–). ^1H NMR ($CDCl_3$, δ in ppm): 0.75–0.82 (m, 9H, CH_3), 0.96–1.48 (m, 27H, CH_2), 4.03 (d, 2H, CH_2OPh), 4.95 (m, 1H, $OCHCH_2$), 7.00–7.02 (d, 2H, aromatic), 7.89–7.98 (m, 4H, aromatic), 8.15–8.17 (d, 2H, aromatic).

2.3. Polymerization

The homopolymer was prepared by radical polymerization in a sealed ampoule tube with 3 mol% of azobisisobutyronitrile (AIBN) in anhydrous benzene at 60 °C for 24 h. The polymer was purified by repeated precipitation with methanol and dried in a vacuum.

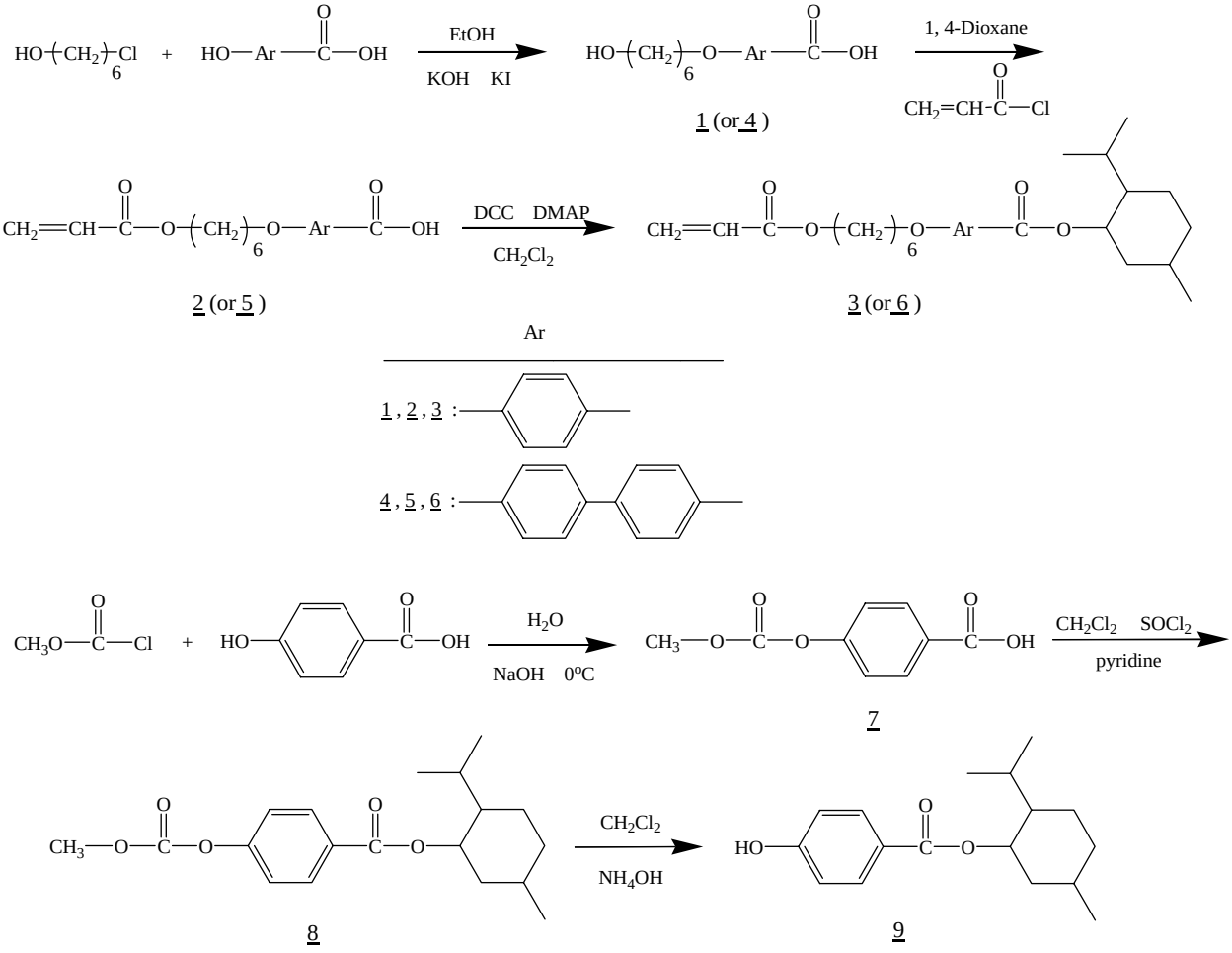

Scheme 2.

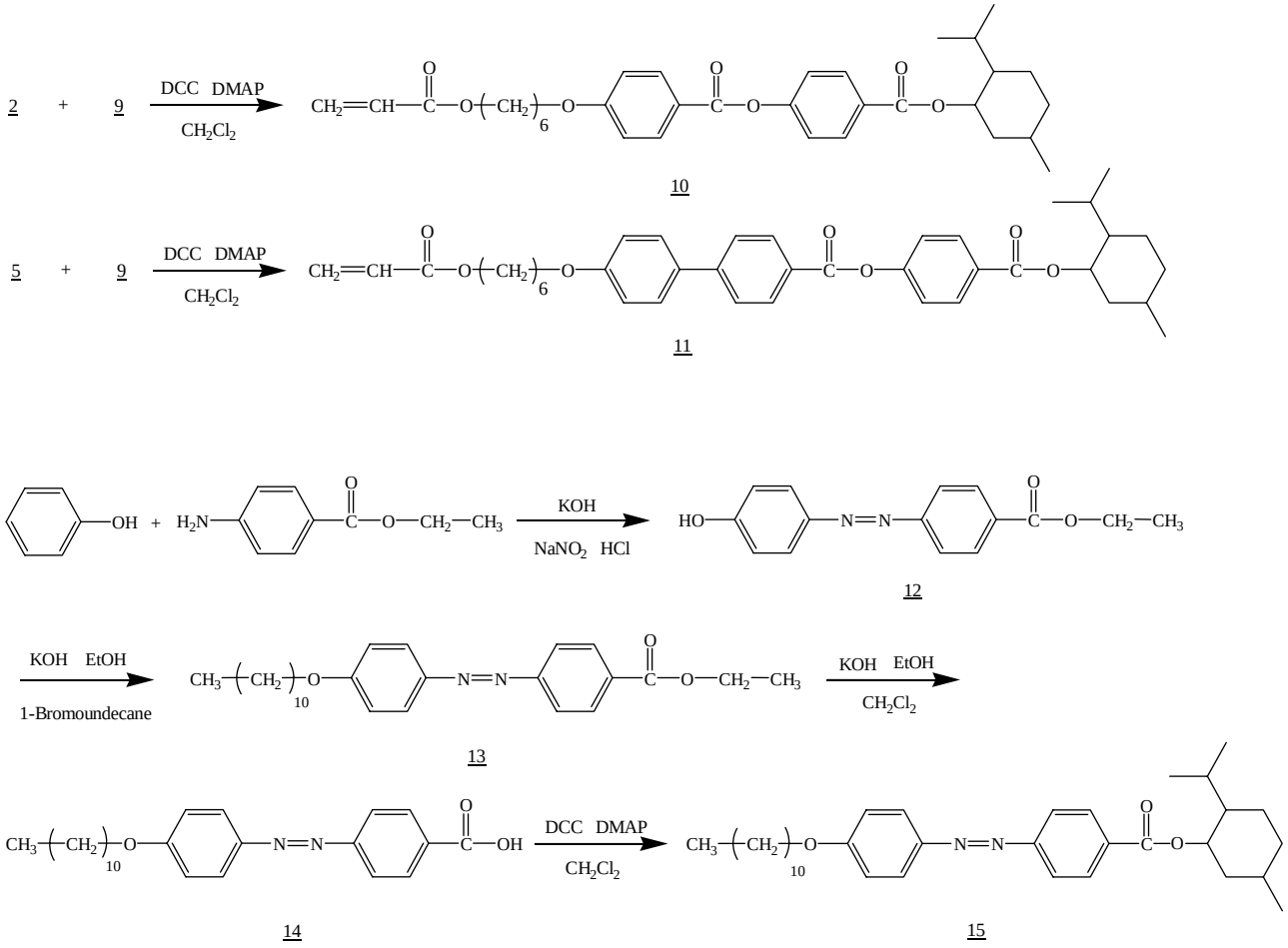

Scheme 3.

2.4. Fabrication of liquid crystal cells

ITO plates were cleaned with a detergent solution, then ultrasonically washed with water followed by acetone, for 20 and 60 min, respectively. The ITO plates were dried in vacuum; one side was coated with polyvinyl alcohol (M_w 520,000), dried and then rubbed to provide a homogeneous alignment. Glass cells, each with a pair of parallel pre-rubbed ITO plates and a 12 μm gap, were fabricated. After it was filled with a cholesteric liquid crystal/monomer/azobisisobutyronitrile (AIBN) mixture, each cell was sealed with epoxy resin. The sealed cell was heated at 90 °C for 1 h to polymerize the monomers. The mixture of commercially available nematic ZLI-2293 with chiral compound **9** (10/3), 4 wt% monomer, and 3 wt% AIBN was used as the composition of the cholesteric liquid crystal cell.

3. Result and discussion

Due to the presence of the molecular chirality, the cholesterically ordered material has regions, which selectively reflect circularly polarized electromagnetic radiation of a band of wavelengths. The central wavelength (λ_0) of the band of reflected wavelengths is determined by the pitch (p) of the molecular helix, according to $\lambda_0 = \bar{n} \times p$, where $\bar{n}$ is the average refractive index of the cholesterically ordered material. The bandwidth $\Delta\lambda$ is given by $\Delta\lambda = p \times \Delta n$, where Δn is the birefringence of the uniaxially oriented phase corresponding to the cholesterically ordered phase. In the visible range, the regions selectively reflect circularly polarized light of a particular color [18,28–30]. (−)-Menthyl group with three chiral centers is expected to reveal high steric effect and affect the pitch of the helical structure of cholesteric liquid crystals.

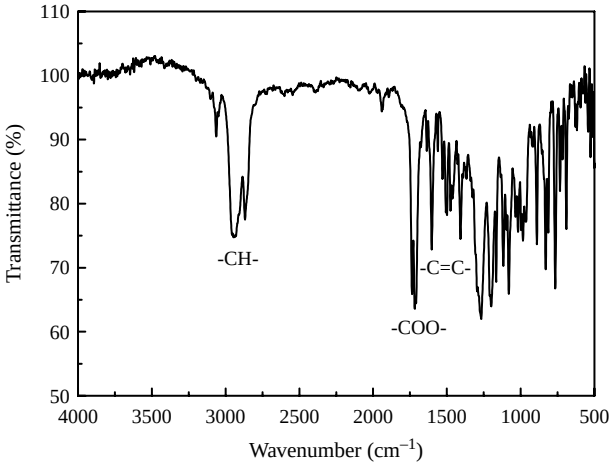

Fig. 1. FTIR spectrum of compound 11 (M4).

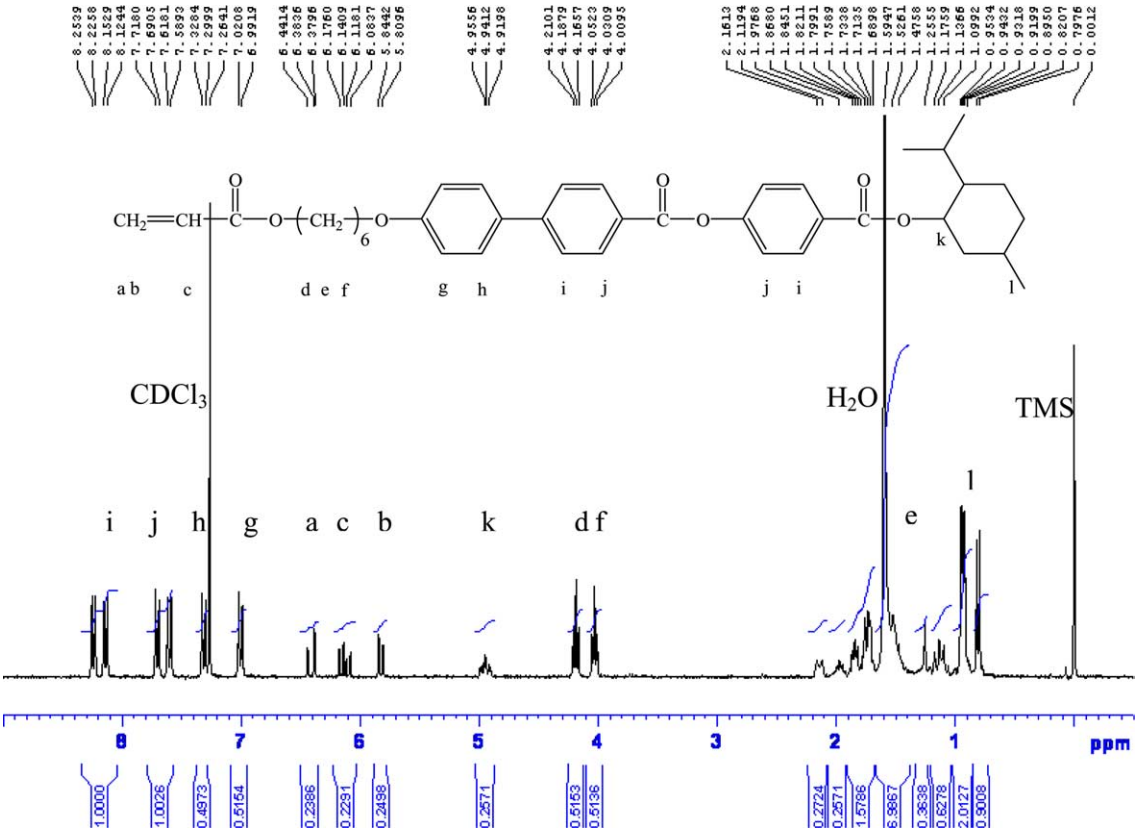

Fig. 2. ^{1}H NMR spectrum of compound 11 (M4) in $CDCl_3$.

To investigate the effect of chiral menthyl unit and the polarity of the chiral molecules on the thermal properties of polymers and the optical behaviors of the cholesteric liquid crystals, a series of monomeric chiral compounds with various spacers and a photoisomerizable azobenzene compound end-caped with (−)-menthyl moiety were synthesized. Scheme 1 shows the structures of the chiral monomers and the azobenzene derivative synthesized in this investigation. Typical synthetic processes of the chiral compounds are shown in Schemes 2 and 3. The synthesized chiral compounds were identified using ^{1}H NMIR, FTIR, and elemental analysis.

The menthyl group was introduced into the monomers through the hydroxyl group of the menthol. The bonds were not broken during the introduction of the menthyl group. Accordingly, the configuration of the introduced menthyl group in the chiral compounds must be retained. Fig. 1 shows the FTIR of compound **11**. The specific split absorptions around 1720 cm^{-1} might be due to the existence of the three carbonyl groups in monomer **11**. Double bond absorption also appeared around 1640 cm^{-1}. Fig. 2 shows the ^{1}H NMR spectrum of compound **11**. Peaks for the protons of the molecule were all identified and shown in the figure. Elemental analyses of the synthesized chiral compounds are summarized in Table 1. To compare with other novel polymers containing pendant (−)-menthol group, polymerization of the monomeric compound **10** and the physical properties of the chiral polymer (P3) were all studied.

The intermediates **2** and **13** were found to have liquid crystal phases. Fig. 3 shows DSC thermograms of compound **13** at a heating rate of 10 °C/min. Compound 13 was found to reveal a mesophase during the cooling cycle. Fig. 4(a) and (b) show the polarized optical microscopic (POM) textures of each of the compounds **2** and **13**. Colorful textures of the mesophases of the compounds were found during heating and cooling for compound **2** and **13**, respectively. The results in Fig. 4 are consistent with those obtained in Fig. 3. According to the textures obtained by the polarizing optical microscope, compound **2** is characterized as a nematic liquid crystal [31]. Fig. 5(a) and (b) show the X-ray pattern of the compounds 2 and 13, respectively. The X-ray pattern of the compound **2**

Table 1
Elemental analysis (EA) of the synthesized compounds

Compound	Formula[a]	EA	C (%)	H (%)	N (%)
M1	$C_{26}H_{38}O_5$	Calcd	72.56	8.84	–
	(430)	Found	72.29	8.83	
M2	$C_{32}H_{42}O_5$	Calcd	75.89	8.30	–
	(506)	Found	75.53	8.34	
M3	$C_{33}H_{42}O_7$	Calcd	72.0	7.64	–
	(550)	Found	72.04	7.81	
M4	$C_{39}H_{46}O_7$	Calcd	74.76	7.35	–
	(626)	Found	74.66	7.43	
AzoM	$C_{34}H_{50}N_2O_3$	Calcd	76.40	9.36	5.24
	(534)	Found	76.12	9.28	5.36

[a] Weight–average molecular weights appear in parentheses.

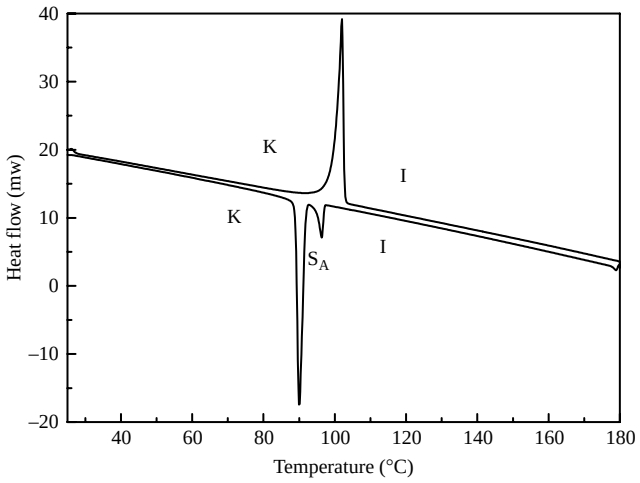

Fig. 3. DSC thermograms of compound 13 at a heating rate of 10 °C/min.

shows a typical nematic characteristics of broad peak in the region $2\theta = 17–30°$, classically due to lateral interference of the mesogenic cores with *d*-spacing of 3–5 Å at 90 °C. The X-ray pattern of the compound 13 shows a sharp peak at $2\theta = 2.86°$, corresponding to the periodic distance and the layer thickness 30.8 Å at 93 °C under cooling. This suggests the layer characteristics of the smectic A (S_A) phase. The *d*-spacing estimated from the X-ray diffraction for liquid crystal phases is

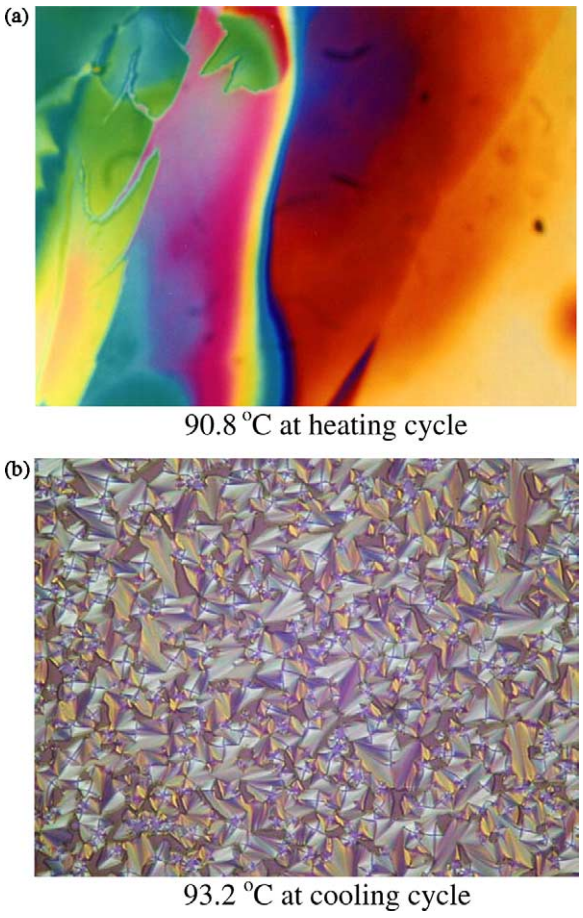

Fig. 4. Polarizing microscopic textures of compound (a) 2, and (b) 13; (×100).

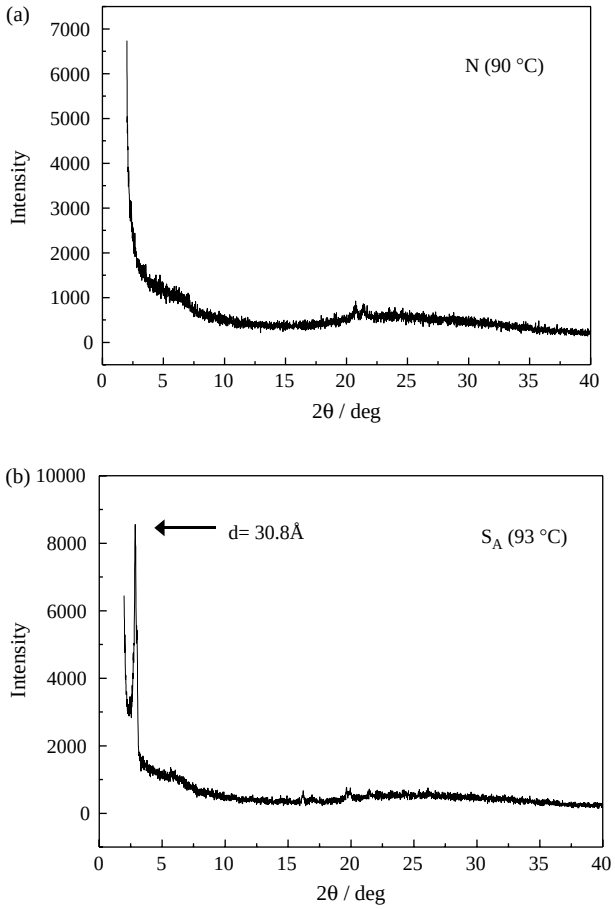

Fig. 5. XRD spectra of compounds (a) 2, and (b) 13.

30.8 Å, which almost coincides with the length of the azobenzene-containing molecule length (about 31.7 Å).

Comparing the molecular structure of **2**, **3** and **13**, **15**, the existence of the menthyl group seems to disturb the arrangement of the molecules. The group volume of menthyl is much higher than that of ethyl. Steric hindered menthyl group might decrease the molecular interaction leading to the disappearance of liquid crystal phases.

The phase transition temperature and specific rotation of the chiral compounds were estimated using a DSC and a polarimeter, respectively. The results are summarized in Table 2. The chiral monomers in Table 2 revealed no liquid crystal phases. In general, liquid crystals must contain suitable

Table 2
Phase transition temperature (°C), enthalpy changes (J/g)[a] and specific rotation of compounds

Sample	Heating cycle[b]	Cooling cycle	$[\alpha]_D^{25}$[c]
M1	K 10.4 (15.6) I	I 0.5 (−6.4) K	−48.3
M2	K 60.5 (108.2) I	I 31.5 (−56.2) K	−38.9
M3	K 32.6 (25.4) I	I 12.5 (−7.9) K	−46.2
M4	K 98.3 (65.6) I	I 43.8 (−2.8) K	−30.8
AzoM	K 71.7 (64.8) I	I 42.8 (−62.4) K	−51.6

[a] Enthalpy of the phase change during heating and cooling at a rate of 10 K min^{-1}.
[b] K, crystal; I, isotropic.
[c] Specific rotation of compounds, 0.1 g in 10 ml $CHCl_3$.

polarity and spacer length at the center and terminals. Furthermore, as can be seen in Table 2, besides monomer 1, the chiral compounds in Table 2 revealed different thermal stabilities with various enthalpies during the heating and cooling cycles. The specific rotation was evaluated at 30 °C in $CHCl_3$ using a Jasco DIP-370 polarimeter with the D-line of sodium ($\lambda = 589$ nm) reading to $\pm 0.001°$. As shown in Table 2, the specific rotations of the chiral compounds are all negative values. As can be seen in Scheme 2, cleavage of O–H bond of (−)-menthol occurred during the introduction of menthyl group into each of the chiral monomers. Accordingly, the configuration of the menthyl groups must be retained for all synthesized chiral compounds in Table 2. As compared with (−)-menthol ($[\alpha] = -50.2°$), compounds **M2** and **M4** bearing a biphenyl segment showed significantly higher specific rotations. The results suggest that the existence of high resonance biphenyl segment might affect the molecule polarity leading to the decrease of the specific rotations.

To study the thermal stability and optical rotation of the chiral polymers, polymerization of the chiral monomers was carried out. The results of the polymerization are summarized in Table 3. Cleavage of the double bond and the binding of other monomers together did not seem to significantly affect the chirality of the compounds. As shown in Table 3, the specific rotation of polymers **P2** and **P4** revealed similar tendency as those described above for **M2** and **M4**. Biphenyl segment in pendant group of polymers might reveal similar polarity effect on the polymers leading to the increase of the specific rotation.

The thermal stabilities of the polymers were estimated using TGA. Fig. 6 shows the results of the TGA curves of the homopolymers. The mass decrease of around 400 and 460 °C may be due to the occurrence of the thermal degradation of the ester/acetate side chain and then the main chain, respectively. As shown in Table 4, **P2** and **P4** polymers revealed relatively higher glass transition temperatures. The existence of a biphenyl segment in **P2** and **P4** might increase the intermolecular π–π interaction between the repeating units. As shown in Table 2, both **M2** and **M4** revealed similar thermal stabilities; and relatively higher melting points were also obtained. The results show that half of the weight loss temperatures of the polymers are higher than 428 °C. It also suggests that the existence of the longer side chain groups may cause a strong interaction between the repeating units and

Table 3
Results of homopolymerization

Polymer	M_w (g mol^{-1})[a]	PDI	Yield (%)[b]	$[\alpha]_D^{25}$[c]
P1	1.2×10^4	2.16	45.5	−45.2
P2	9.9×10^3	2.29	53.6	−37.8
P3	1.7×10^4	2.45	57.2	−44.5
P4	1.2×10^4	2.21	72.1	−25.3

M_w, weight–average molecular weight; M_n, number-average molecular weight; PDI, polydispersity index (M_w/M_n).
[a] Measured by GPC with a polystyrene standard.
[b] Isolated yield.
[c] Specific rotation, 1.0 g in 100 ml $CHCl_3$.

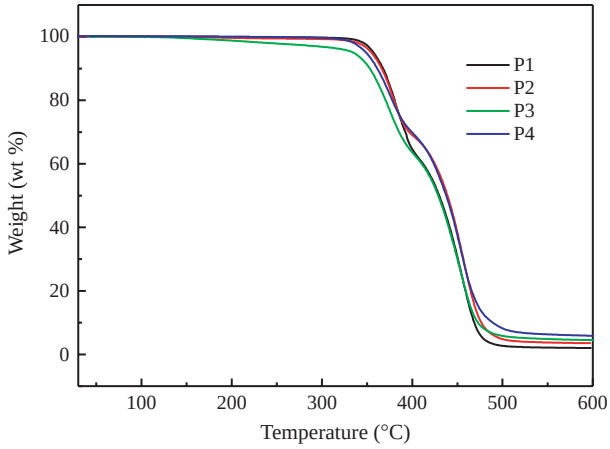

Fig. 6. TGA curve of homopolymer P1–P4.

entanglement of the polymer chains. The strong interaction between the chiral repeating units is expected to raise the interaction between the liquid crystal and the polymers leading to an increase in the stabilization of liquid crystals inside the polymer matrix.

As can be seen in Scheme 1, chiral **AzoM** contains an azo structure in the middle section. As shown in Fig. 7(a), UV irradiation caused the configurational variation of the molecule from *E* to *Z* leading to an increase and a decrease in the spectra absorption around 360 and 450 nm, respectively. **AzoM** in the *E* form showed a strong absorbing band in the UV-region (∼360 nm) which is attributed to the π–π* transition, and a weak absorbing band in the visible region (∼450 nm) due to the *n*–π* transition. The *E* form is generally more stable than the *Z* form, but each isomer can be converted into the other by light irradiation of the appropriate wavelength. Fig. 7(b) shows the stability of **AzoM** in the dark environment at 25 °C. After 24 h, the **AzoM** molecule returned to its original absorption level. The results suggest that the *Z*-form of **AzoM** changed graduate to *E*-form without any light exposure. Addition of **AzoM** into cholesteric liquid crystal cells is expected to reveal photoisomerization. According to the theory, UV induced configurational E–Z isomerization is able to alternate the pitch of the helical structure of the cholesteric liquid crystal.

The liquid crystal cell with the mixture of commercially available nematic ZLI-2293 with chiral compound **9** (10/3), 4 wt% monomer 2 (**M2**) and 3 wt% AIBN was heated at 90 °C for 1 h. Optical properties of the fabricated cholesteric liquid

Table 4
Thermal properties of polymers

Polymer	T_g[a] (°C)	TGA[b]		
		5% Weight loss temperature (°C)	10% Weight loss temperature (°C)	50% Weight loss temperature (°C)
P1	37.7	357.2	368.0	429.9
P2	58.3	355.0	366.1	439.0
P3	33.7	334.8	353.1	428.7
P4	63.7	349.2	363.1	437.5

[a] Estimated during the second heating scan at a heating rate of 10 °C min^{-1} in nitrogen.
[b] Measured at a heating rate of 40 °C min^{-1}.

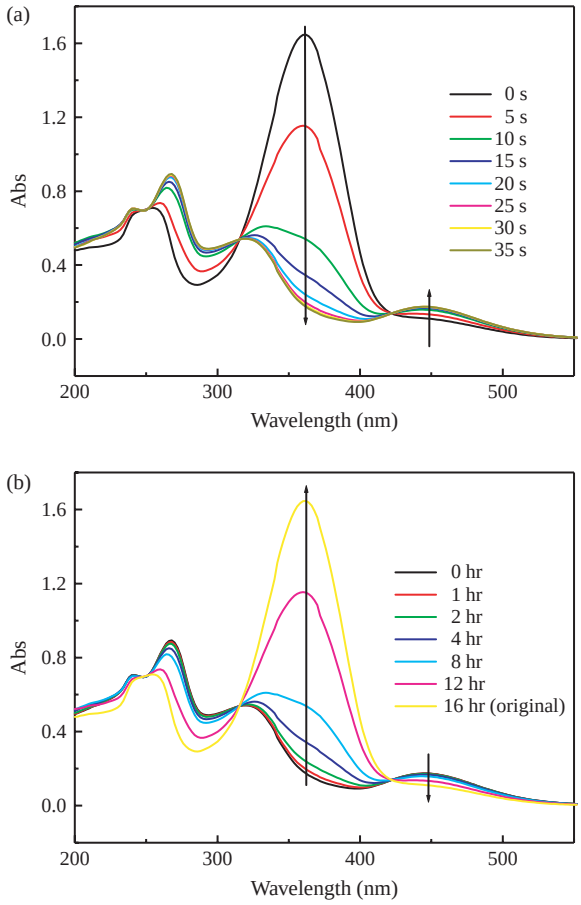

Fig. 7. UV spectra of compound 15 in chloroform before and after UV irradiation.

crystal cells were investigated. Fig. 8 shows the reflective band of the liquid crystal cell induced by the chiral dopant of compound **9** inside polymer 2 (**P2**) matrix. As can be seen, increase of the molar ratio of chiral dopant 9 in liquid crystal decreases the pitch of the cholesteric liquid crystal leading to the blue shift. The appearances of the cells are colorful, which

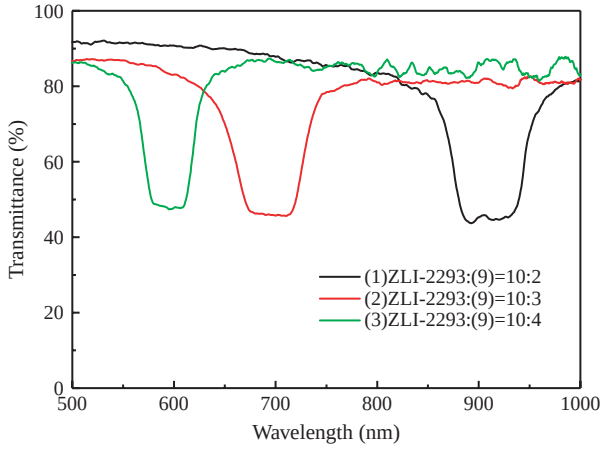

Fig. 8. Reflective band of cholesteric liquid crystal cells with various molar ratio of chiral compound (9).

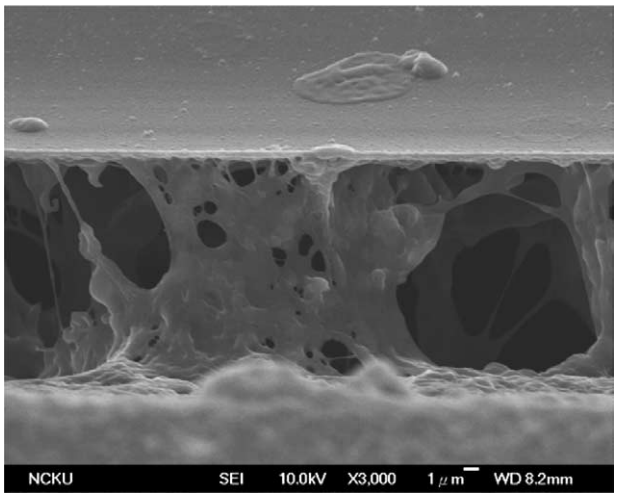

Fig. 9. Side view of morphological network structure of a cholesteric liquid crystal cell.

revealed reflective bands 1 and 2 in the visible region. They are available as reflective polarized color filters. Furthermore, the cell reflected band 3 is expected to be useful in the field of thermal shielding materials. To investigate the morphology of the polymer matrix, after polymerization, the cell glasses were opened along the crossed direction with a diamond cutter. The liquid crystals were washed out thoroughly using *n*-hexane. Fig. 9 shows the scanning electron microscope (SEM) photograph of the side view of the morphological network structure of a cholesteric liquid crystal cell. Liquid crystals were separated and stabilized inside the polymer matrix. The polymer matrix is expected to fix the cell gap between the substrates, especially for the flexible liquid crystal films.

Further more, the photochemical tuning capability of the cholesteric liquid crystal cell with AzoM was evaluated. In Fig. 10, curve (a) shows the chiral effect of AzoM on the cholesteric liquid crystal cell. Addition of 0.5 wt% AzoM into the host of ZLI-2293/(9) = 10/4 may increase the chiral effect of chiral dopants. The blue shift reveals that the pitch of

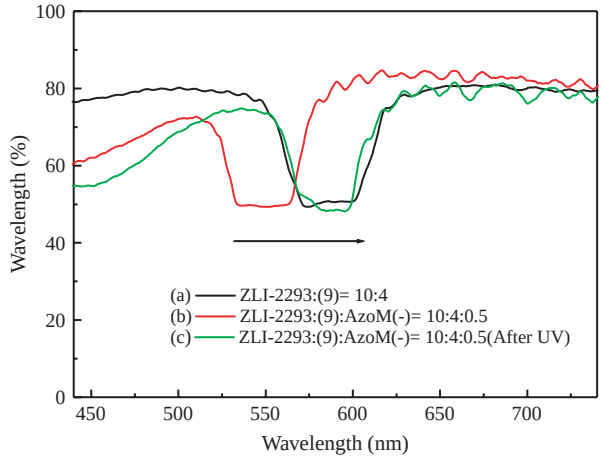

Fig. 10. Effects of UV irradiation at room temperature on cholesteric cells with AzoM. (ZLI-2293/(9)/AzoM = 10/4/0.5).

the cholesteric liquid crystal was reduced. However, after UV ($\lambda = 365$ nm) irradiation [curve (c) in Fig. 10] the *E/Z* configurational change of AzoM might expand the pitch of the cholesteric liquid crystal thereby leading to a red shift. The phototuning ability of the AzoM will be useful in the designing of the photo-recordable material.

4. Conclusion

A series of monomeric chiral compounds with various spacers and a photoisomerizable azobenzene compound, which were all end-capped with (−)-menthyl moiety were synthesized. Homopolymerization of the chiral monomers were carried out. The thermal properties of the monomers and polymers were estimated. It was found that the configuration of the introduced menthyl group in the chiral compounds was retained. A high resonance biphenyl segment decreased the absolute value of the specific rotation of the chiral monomers **M2** and **M4**. The existence of a biphenyl segment in **P2** and **P4** might increase the molecular interaction between the repeating units leading to the increase of the thermal resistance of the polymers. UV irradiation caused the E/Z isomerization of AzoM leading to the variation of UV–vis spectrum around 360 and 450 nm. The chiral compounds and polymers synthesized in this investigation were found to induce the helical structure of the cholesteric liquid crystal phases and stabilize the liquid crystals. The phototuning ability of the AzoM was also confirmed.

Acknowledgements

The authors would like to thank the National Science Council (NSC) of the Republic of China (Taiwan) for financially supporting this research under Contract No. NSC 94-2216-E006-038.

References

[1] Finkelmann H, Ringsdorf H, Wendorff JH. Makromol Chem 1978;179:273. Ichimura K. Chem Rev 2000;100:1847.
[2] Suzuki K, Saito H, Tokita M, Watanabe J. Polymer 2005;46:8313.
[3] Van De Witte P, Galan JC, Lub J. Liq Cryst 1998;24:819.
[4] Meyer JG, Ruhmann R, Sumpe J. Macromolecules 2000;33:843.
[5] Bobrovsky AYu, Boiko NI, Shibaev VP, Springer J. Adv Mater 2000;12:1180.
[6] Zhao Y, Yuan G, Roche P. Polymer 1999;40:3025.
[7] Natansohn A, Rochon P, Meng X, Barret C, Buffeteau T, Bonenfant S, et al. Macromolecules 1998;31:1155.
[8] Kricheldof HR, Wulff DF. Polymer 1998;39:6145.
[9] Ruslim C, Ichimura K. J Phys Chem B 2000;104:6529.
[10] Kurihara S, Nomiyama S, Nonaka T. Chem Mater 2001;(13):1992.
[11] Cowie JMG, Hinchcliffe T. Polymer 1996;37:4937.
[12] Shibaev VP, Bobrovsky A, Boiko N. Prog Polym Sci 2003;(28):729.
[13] Bobrovsky AYu, Boiko NI, Shibaev VP. Polym Sci A 1998;40:232.
[14] Sackmann E. J Am Chem Soc 1971;93:7088.
[15] Ruslim C, Ichimura K. J Mater Chem 2002;12:3377.
[16] Stegmeryer H, Mainush KJ. Naturwissenschaften 1971;58:599.
[17] Sackman E, Meiboom S, Snyder LC, Meixner AE, Dietz RE. J Am Chem Soc 1968;90:3567.
[18] Lee HK, Doi K, Harada H, Tsutsumi O, Kanazawa A, Shiono T, et al. J Phys Chem B 2000;104:7023.
[19] Liu JH, Hsieh CD, Wang HY. J Polym Sci A 2004;(42):1075.
[20] Liu JH, Chen WT, Wu FT. J Polym Res 2002;9:251.
[21] Liu JH, Wang HY. J Appl Polym Sci 2004;9:789.
[22] Liu JH, Yang PC. J Appl Polym Sci 2004;91:3693.
[23] Bobrovsky AY, Boiko NI, Shibaev VP. Liq Cryst 1998;24:489.
[24] Hattori H, Uryu T. Liq Cryst 1999;(26):1085.
[25] Liu JH, Hsieh CD, Wang HY. J Polym Sci, Part A: Polym Chem 2004;42:1075.
[26] Portugall M, Ringsdorf H, Zentel R. Makromol Chem 1982;183:2311.
[27] Kašpar M, Hamplová V, Pakhomov SA, Bubnov AM, Guittard F, Sverenyák H, et al. Liq Cryst 1998;24:599.
[28] Tamaoki N, Parfenov AV, Masaki A, Matsuda H. Adv Mater 1997;9:1102.
[29] Brehmer M, Lub J, Van De Witte P. Adv Mater 1998;10:1438.
[30] Demus D, Goodby J, Grey G, Spiess H, Vill V, editors. Handbook of liquid crystals. New York: Wiley; 1998.
[31] Ingo D. Textures of liquid crystals. Weinheim: Wiley-VCH; 2003 [ISBN 3-527-30725-7].